AAS 20-061

PROSPECTS AND CHALLENGES FOR MAGNETIC PROPELLANT POSITIONING IN LOW-GRAVITY

Álvaro Romero-Calvo,* Filippo Maggi† and Hanspeter Schaub‡

The sloshing of liquids in low-gravity entails several technical challenges for spacecraft designers and operators. Those include the generation of significant attitude disturbances, the uncontrolled displacement of the center of mass of the vehicle or the production of gas bubbles, among others. Magnetic fields can be used to control the position of a magnetically susceptible propellant and transform a highly stochastic fluid system (non-linear sloshing) into a deterministic problem (linear sloshing). The employment of magnetic settling forces also produces an increase of the natural sloshing frequencies and damping ratios of the liquid. Despite being proposed in the early 1960s, this approach remains largely unexplored. A recently developed magnetic sloshing control model is here presented and extended, and potential space applications are explored. Technical challenges associated with the reachability, scaling and stability of paramagnetic and ferromagnetic systems are discussed, unveiling a roadmap for the implementation of this technology.

INTRODUCTION

Propellant sloshing has historically represented a major concern for aerospace engineers due to its capacity to disturb the dynamics of space vehicles. During launch, the uncontrolled movement of liquids may lead to a total or partial mission failure.[1] In microgravity, sloshing is characterized by its highly stochastic nature, which results in a complicated propellant management system design and an additional disturbance for the attitude control system of the spacecraft.[2] Propellant Management Devices (PMD) are commonly employed to ensure a gas-free expulsion of propellant, fix the center of mass of the fluid and increase the sloshing frequencies and damping ratios. However, they also increment the inert mass of the vehicle and complicate numerical simulations.[3,4]

An interesting alternative to classical PMDs and active settling methods would be the employment of electromagnetic fields to generate a gravity-equivalent force. The use of *dielectrophoresis*, a phenomenon on which an electric force is exerted on dielectric materials, was explored by the US Air Force with suitable propellants in 1963. The study unveiled a high risk of arcing inside the tanks and highlighted the need for large, heavy and noisy power sources.[5] The magnetic equivalent, named *Magnetic Propellant Positioning* (MP^2), has also been suggested to exploit the inherent properties of paramagnetic and diamagnetic liquids.[6]

MP^2 devices must deal with the rapid decay of magnetic fields with distance, that limits their applicability to relatively small regions. This difficulty may be compensated by employing highly susceptible materials. Ferrofluids are colloidal suspensions of magnetic nanoparticles developed in the early 1960s to enhance the susceptibility of rocket propellants.[6] Despite having numerous applications on Earth, contributions addressing their original purpose are scarce. High-gravity works have explored the natural frequency shifts due to the magnetic interaction,[7] axisymmetric sloshing,[8,9] two-layer sloshing,[10] liquid swirling[11] or the development of tuned magnetic liquid dampers.[12,13] Low-gravity contributions include the gravity compensation

* Graduate Research Assistant, Department of Aerospace Engineering Sciences, University of Colorado, 431 UCB, Colorado Center for Astrodynamics Research, Boulder, Colorado 80309-0431, USA.
E-mail: alvaro.romerocalvo@colorado.edu.
† Professor, Department of Aerospace Science and Technology, Politecnico di Milano, Space Propulsion Laboratory, Via Giuseppe La Masa, 34, 20156, Milan, Italy.
‡ Professor, Glenn L. Murphy Chair, Department of Aerospace Engineering Sciences, University of Colorado, 431 UCB, Colorado Center for Astrodynamics Research, Boulder, Colorado 80309-0431, USA. AAS Fellow.

experiments performed by Dodge in 1972. These indirectly addressed the low-gravity sloshing of ferrofluids subjected to quasi-uniform magnetic forces.[14] Motivated by the advent of stronger permanent magnets and high-temperature superconductors, the NASA MAPO experiment validated the magnetic positioning of liquid oxygen in a series of parabolic flights in 2001.[15] Subsequent publications present refined numerical models to study this phenomenon.[16–20] The axisymmetric sloshing of water-based ferrofluids was characterized in microgravity when subjected to an inhomogeneous magnetic field as part of the ESA Drop Your Thesis! 2017 campaign.[21,22] As a follow-up, the lateral sloshing of ferrofluids was studied in the framework of the UNOOSA DropTES Programme 2019.[23,24] A recent quasi-analytical model addresses the free and forced oscillations of magnetic liquids in axisymmetric containers when subjected to inhomogeneous magnetic fields in low-gravity.[25] The problem is faced assuming small oscillations, naturally leading to the employment of quasi-analytical procedures and simplified mechanical analogies.

This paper summarizes the basic theoretical framework introduced in Ref. 25, presents a series of representative space applications dealing with the magnetic control of space propellants and describes the most important technical challenges of this technology. Although ferrofluids are preferred due to their enhanced magnetic properties, any kind of magnetic liquid may be potentially employed in this framework

MAGNETIC SLOSHING MODEL

This section overviews the theoretical framework to study the low-gravity sloshing of magnetic liquids in axisymmetric tanks. Computationally efficient quasi-analytic tools are preferred over purely numerical solutions, as they provide further insight into the physics of the system. Complex configurations of geometries and loads may require ferrohydrodynamic computational models instead.[15,20] The subsections concerning the determination of the magnetic equilibrium surface (meniscus) and modal frequencies are summarized from Ref. 25.

The axisymmetric propellant tank under analysis is represented in Fig. 1. A volume V of magnetic propellant fills the container and develops a meniscus with contour radius a in microgravity. The liquid is incompressible, Newtonian, with density ρ, kinematic viscosity ν, surface tension σ, and wall contact angle θ_c. An applied inhomogeneous axisymmetric magnetic field $\boldsymbol{H}_0$ is imposed by a magnetic source located at the base of the vessel and interacts with the fluid with magnetization $M(H)$. H and M are the modules of the collinear magnetic $\boldsymbol{H}$ and magnetization $\boldsymbol{M}$ fields, respectively. A non-reactive gas at pressure p_g fills the free space. In the figure, s is a curvilinear coordinate along the meniscus with origin in the vertex O and the relative heights are w (fluid surface - vertex), f (meniscus - vertex) and h (fluid surface - meniscus).

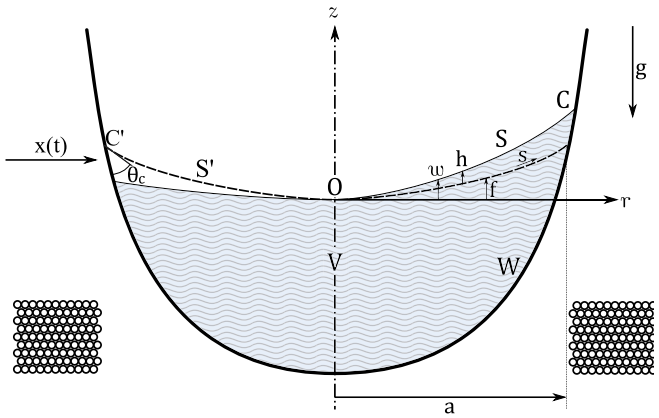

Figure 1: Geometry of the system. S' refers to the fluid surface, S is the equilibrium meniscus, O denotes the vertex of the equilibrium surface, C is the fluid surface contour, W is the vessel wall and V is the fluid volume.[25]

Magnetic meniscus profile

The axisymmetric meniscus profile can be determined from the balance of vertical forces in a segment of the surface, resulting in the set of dimensionless differential equations[25]

$$\frac{\mathrm{d}}{\mathrm{d}\mathcal{S}}\left(R\frac{\mathrm{d}F}{\mathrm{d}\mathcal{S}}\right) = R\frac{\mathrm{d}R}{\mathrm{d}\mathcal{S}}\left[\lambda + BoF - \overline{\psi}(R)\right], \tag{1a}$$

$$\frac{\mathrm{d}F}{\mathrm{d}\mathcal{S}}\frac{\mathrm{d}^2F}{\mathrm{d}\mathcal{S}^2} + \frac{\mathrm{d}R}{\mathrm{d}\mathcal{S}}\frac{\mathrm{d}^2R}{\mathrm{d}\mathcal{S}^2} = 0, \tag{1b}$$

and boundary conditions

$$R(0) = F(0) = \frac{\mathrm{d}F(0)}{\mathrm{d}\mathcal{S}} = 0,\ \frac{\mathrm{d}R(0)}{\mathrm{d}\mathcal{S}} = 1, \tag{1c}$$

$$\frac{\mathrm{d}F(1)}{\mathrm{d}R} = \tan\left(\frac{\pi}{2} - \theta_c\right), \tag{1d}$$

where $R = r/a$, $\mathcal{S} = s/a$, $F = f/a$, $Bo = \rho g a^2/\sigma$ is the Bond number, $\lambda = a(p_g - p_0)/\sigma$, being p_0 the liquid pressure at the free surface vertex, and $\overline{\psi}$ includes the magnetic terms through

$$\overline{\psi}(R) = \frac{a\mu_0}{\sigma}\left[\int_{H(0,0)}^{H(R,F(R))} M(H)\mathrm{d}H + \frac{\mathrm{M}_n^2}{2}\right]_{F(R)}, \tag{2}$$

with $\mu_0 = 4\pi \cdot 10^{-7}$ N/A^2 being the permeability of free space. Starting from an initial guess, the system is solved by (i) defining an initial vertex position, (ii) computing the value of λ iteratively in order to satisfy the contact angle condition given by Eq. (1d), (iii) solving the system with an ODE solver, (iv) applying volume conservation to obtain the new height of the vertex, and (v) recomputing the fields $\boldsymbol{H}$ and $\boldsymbol{M}$ with the new geometry. The procedure is repeated until the surface converges with the desired accuracy. Alternative formulations of Eqs. (1) can be developed by following the procedures described in the bibliography.[26]

Determination of critical loads

Under certain circumstances, the combined action of surface tension and magnetic forces can compensate an adverse inertial acceleration and keep the meniscus stable. The *critical Bond number* Bo^* is associated to the value of negative acceleration that destabilizes the surface.[26] This is an important parameter for space applications due to its capacity of establishing an upper disturbance limit and driving the design of the liquid management system.[2,3] Although the non-magnetic problem has raised significant attention since the Apollo era, its magnetic equivalent remains unexplored.

Referring to Myshkis, *if for a certain position of absolute equilibrium of a liquid the second variation $\delta^2\mathcal{U}$ of the potential energy $\mathcal{U}$ for the mechanical system "liquid + vessel wall" is positive, the position will be stable*.[26] Consequently, the stability analysis relies in the study of the potential energy associated to the meniscus, given by

$$\mathcal{U} = \sigma|S| + \tilde{\sigma}|W| + \sigma_g|W_g| + \rho\int_V \Pi dV, \tag{3}$$

where $\tilde{\sigma}$ and σ_g are respectively the surface tensions of the pairs liquid/wall and gas/wall, the gas is denoted by the subscript g, $|\cdot|$ represents the area of the corresponding surface and Π is the mass-force field potential.

Before writing the magnetic terms of Π, it is convenient to discuss the physical nature of the magnetic interaction. According to the classical literature, magnetic fluids in the presence of inhomogeneous magnetic fields are subjected to a volume force density $\mu_0\boldsymbol{M}\nabla\boldsymbol{H}$ and a *magnetic normal traction* $\mu_0\mathrm{M}_n^2/2$ at the surface, where M_n is the normal magnetization component.[27] The volume contribution derives from a potential under the assumption of isothermal flow.[28] A rigorous treatment of the problem should include this term in the mass-force field potential Π and the surface pressure both in the potential definition and interface boundary condition. However, this approach complicates the derivation of analytical results.

Alternatively, an equivalent local force may be defined after integrating both components in the fluid volume and applying the Divergence Theorem, resulting in[29]

$$\boldsymbol{f}_m = \mu_0(\boldsymbol{M}\cdot\nabla)\boldsymbol{H} + \frac{\mu_0}{2}\nabla(M_n^2). \tag{4}$$

Under the framework of analysis established by the classical literature,[27] this expression does not reflect the actual local force acting in the medium (known as Kelvin force). However, Petit *et al.* show that it has the best agreement with virtual work method simulations,[29] reflecting the intense historical debate that surrounds the proper formulation of the magnetic force distribution on highly susceptible magnetic fluids, such as ferrofluids.[30–32] Independently of this discussion, the force density given by Eq. 4 allows treating volume and surface terms as a mass-force potential of the form[28]

$$\Pi = gz + \Pi_m, \quad \text{with} \quad \Pi_m = -\int_0^H M(H)dH - \frac{M_n^2}{2}, \tag{5}$$

where Π_m is defined with a negative sign ($f_m = -\nabla\Pi_m$). In other words, the results from the classical low-gravity fluid mechanics theory[26] can be used directly with this approximate potential. When the liquid has a large magnetic susceptibility, FEM-in-the-loop simulations become necessary to compute the magnetic fields $\boldsymbol{H}$ and $\boldsymbol{M}$.

As a final remark, it should be noted that the discussion on the proper formulation of the local force density lacks of practical interest for low magnetic susceptibilities ($\chi \ll 1$). The relative importance of the surface component becomes negligible in those cases and the potential reduces to the integral term in Eq. 5.

Modal analysis

The free and forced oscillations of the free surface can be analyzed through modal analysis as described in Ref. 25. This magnetic sloshing model assumes inviscid, potential, isothermal, magnetically dilluted flow and extends the works by Satterlee & Reynolds[33] and Yeh[34] by considering the magnetic interaction. The sloshing eigenfrequencies and eigenmodes can be then computed after linearizing around the meniscus by solving the variational principle

$$\begin{aligned} I = &\iint_{S'}\left[\frac{\mathcal{H}_R^2}{(1+F_R^2)^{3/2}} + \frac{1}{R^2}\frac{\mathcal{H}_\theta^2}{(1+F_R^2)^{1/2}} + (Bo + Bo_{\text{mag}}(R))\,\mathcal{H}^2 - \Omega^2\Phi\mathcal{H}\right]RdRd\theta \\ &- \Omega^2\iint_W \Phi G R dR d\theta - \Gamma\int_{C'}\left[\frac{\mathcal{H}^2}{(1+F_R^2)^{3/2}}\right]_{R=1}\mathrm{d}\theta \\ &= \text{extremum}, \end{aligned} \tag{6a}$$

subjected to

$$\nabla^2\Phi = 0 \text{ in } V, \tag{6b}$$

$$\mathcal{H} = \Phi_Z - F_R\Phi_R \text{ on } S', \tag{6c}$$

$$G = \Phi_Z - W_R\Phi_R \text{ on } W, \tag{6d}$$

$$\mathcal{H}_R = \Gamma\mathcal{H} \text{ on } C', \tag{6e}$$

where the subindices denote the partial derivatives and the magnetic Bond number is defined as

$$Bo_{\text{mag}}(R) = -\frac{\mu_0 a^2}{\sigma}\left(M\frac{\partial H}{\partial z} + \mathrm{M}_n\frac{\partial \mathrm{M}_n}{\partial z}\right)_{F(R)}, \tag{7}$$

and describes the effects of the external magnetic field on the liquid with respect to surface tension. The dimensionless variables $R = r/a$, $Z = z/a$, $F = f/a$, $\phi(R,\theta,Z,t) = \sqrt{g_0 a^3}\Phi(R,\theta,Z)\sin(\omega t)$, $h(R,\theta,t) = \sqrt{ag_0/\omega^2}\mathcal{H}(R,\theta)\cos(\omega t)$, $\Omega^2 = \rho a^3\omega^2/\sigma$, $\Gamma = a\gamma$ are employed with g_0 being the acceleration of gravity

at ground level, ϕ the perturbed velocity potential, ω the circular frequency, γ the hysteresis condition parameter and $\{r, \theta, z\}$ a set of cylindrical coordinates with center in the vertex of the meniscus. The *free-edge* condition is characterized by $\gamma = 0$, while the *stuck-edge* condition is associated to $\gamma \to \infty$. G accounts for the non-penetration wall boundary condition as described in Ref. 34.

Once the axisymmetric meniscus S', defined by the curve $F(R)$, is determined, the system described by Eqs. (6) can be solved to obtain the modal frequencies and shapes by following Ritz's method. The development of mechanical analogies to perform attitude dynamics simulations arise naturally from this result. The reader is referred to Ref. 25 for further details on the solution procedure.

Viscosity and damping ratio of ferrofluids

An increase in liquid viscosity leads to higher damping ratios and lower oscillation frequencies. Unlike magnetorheological fluids, ferrofluids retain liquid flowability in the presence of strong magnetic fields. However, their rheology is still affected, impacting on the sloshing problem.

In the absence of magnetic fields, the addition of magnetic particles increases the viscosity η of a ferrofluid with respect to the viscosity of the carrier η_0 by following[27]

$$\frac{\eta - \eta_0}{\phi\eta} = \frac{5}{2}\left(1 + \frac{\delta}{r}\right)^3 - \left(\frac{\frac{5}{2}\phi_c - 1}{\phi_c^2}\right)\left(1 + \frac{\delta}{r}\right)^6 \phi, \tag{8}$$

where ϕ is the solids fraction, $\phi_c = 0.74$ is the concentration of close packing of spheres (at which the suspension becomes rigid), r is the radius of the uncoated particles and δ is the thickness of the surfactant layer covering the ferrofluid nanoparticles.

The application of an external magnetic field aligns the magnetic particles with the field lines. Larger velocity gradients consequently appear in their surroundings, increasing viscous dissipation. According to Shliomis, the magnetic contribution to viscosity is maximized when the directions of the vorticity vector and magnetic field lines are perpendicular, becoming zero if they are parallel. This follows from the relation

$$\frac{\Delta\eta}{\zeta} = \frac{\mu_0 M_0 H\tau}{4\zeta + \mu_0 M_0 H\tau}\sin^2\beta, \tag{9}$$

where ζ is a coefficient named *vortex viscosity*, τ is the *relaxation time constant*, M_0 is the unperturbed magnetization value and β is the angle between the magnetic field $\boldsymbol{H}$ and the vorticity vector Ω.[27,35] An upper viscosity limit can be computed by setting $\beta = \pi/2$. For cases with high shear rate, associated with strong magnetic fields, Shen provides an updated formulation.[36]

APPLICATIONS

The ability of controlling liquids by means of magnetic fields leads to a myriad of exciting applications in space. Those include, but are not restricted to, mass transport,[37] thermomagnetic convection,[38,39] or micropropulsion.[40,41] This section briefly describes three potential propellant management concepts.

Passive magnetic positive positioning (MP^2)

Ferrofluids were developed in the 1960s to enhance the magnetic susceptibility of rocket propellants, which may be (i) satisfactorily oriented in microgravity, (ii) subjected to an artificial gravity condition, and (iii) employed for continuous and easy pumping.[6] The passive MP^2 framework was explored with ferrofluids in the NASA MAPO experiment[15] and subsequent publications addressed applications for liquid oxygen and liquid hydrogen.[16–20]

A magnetic source (e.g. a ring magnet) may be placed in the fuel outlet of a propellant tank to ensure a continuous gas-free supply to the engines. This would replace or complement the existing surface-tension-based PMDs, which add inert mass to the system and complicate numerical analysis. To the best knowledge of the authors, and in spite of the existence of relevant literature on the topic, actual solutions have not yet been developed.

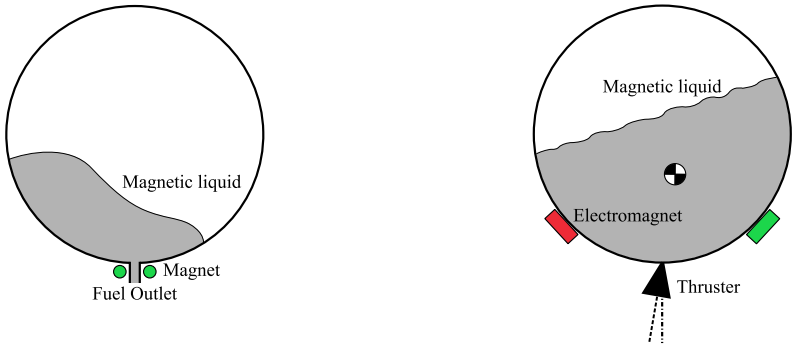

(a) Passive MP^2 (b) Active MP^2

Figure 2: Conceptual representation of passive and active MP^2 devices

Active magnetic positive positioning (MP^2)

A logical evolution of the previous concept is the active propellant management system represented in Figure 2. By making use of a series of strategically located electromagnets, the center of mass of the liquid (and hence, of the spacecraft) may be displaced to the most convenient position. That may serve to correct a potential thrust vector misalignment or generate a prescribed torque during a ΔV firing.

A dedicated analysis must be performed in order to asses the feasibility of the system. The existence of an imposed inertial acceleration increases the magnetic control requirements, leads to higher electromagnet mass and/or current requirements and restricts the range of application of this technology. Moreover, significant uncertainties should be expected in the estimation and control of the center of mass position.

Numerical models are needed to study this non-axisymmetric problem. However, the critical thrust level that destabilizes a magnetically positioned surface can be computed from the previously introduced theoretical framework.

Magnetic sloshing control

As described in Ref. 25, a third representative application may seek to develop an overall magnetic sloshing control system. By employing sufficiently powerful magnetic sources it is possible to reach a significant portion of the tank volume and modify the liquid response to external disturbances. According to the magnetic sloshing model here presented, the addition of a magnetic source would (i) increase the Bo^* value, making the fluid surface less sensitive to external disturbances, (ii) raise the natural sloshing frequencies and damping ratios and, most importantly, (iii) make the system predictable and easily analyzable by means of standard mechanical analogies like the example given in Figure 3 (common in normal-gravity applications). An external controller would then be able to predict and compensate the disturbance torque produced by the liquid, improving pointing accuracy and reducing attitude disturbances.

CHALLENGES

The challenges associated to the practical implementation of the magnetic propellant control concept in space span from purely physical considerations up to the certification process. This section focuses on the physical limitations of the system and the specific difficulties faced by ferrofluid-based propellants.

For illustrative purposes, a liquid oxygen (O_2) / liquid methane (CH_4) in-space bipropellant propulsion system is considered. This combination has been proposed as a green, long-life and compact enabler for future space exploration with in-situ propellant production.[46] An hypothetical liquid methane ferrrofluid with a 0.53% volume concentration of Fe_3O_4 nanoparticles is assumed. This represents a low concentration value

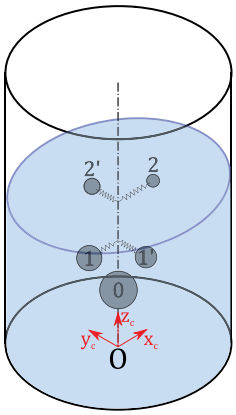

Figure 3: Modal spring-mass mechanical analogy for inviscid liquid sloshing.

in comparison with commercial light-hydrocarbon ferrofluids ($\approx 18\%$, Ferrotec EMG-900) but still produces a significant magnetic response without compromising the performance of the propulsion system.

The physical properties of O_2 (l) and CH_4 (l) + Fe_3O_4 (s) are given in Table 1, with the magnetization curves being represented in Figure 4. The magnetic behavior of the hypothetical CH_4-based ferrofluid is assumed to be equivalent to the 1:10 volume solution of the Ferrotec EMG-700 ferrofluid employed in Ref. 25. While the increase in density due to the addition of nanoparticles is taken into account, the surface tension of CH_4 is considered to remain unaltered.

Filling ratio dependence

The filling ratio (FR), usually defined as the portion of the total height or volume of the container occupied by the liquid, is a relevant parameter in the computation of the modes and equivalent mechanical analogies of a fluid system.[47] This dependence is further complicated by the addition of magnetic sources, that increase the oscillation frequencies and generate a complex meniscus.[25] The accurate modeling of this effect is a key step towards the previous applications and the definition of their operational environment.

Unlike non-magnetic sloshing, a direct generalization of the magnetic sloshing results cannot be easily achieved due to the inhomogeneity of the fields involved. In other words, specific configurations have to be analyzed with specific simulations. A case of analysis is here presented for the aforementioned O_2(l)/CH_4(l) combination. Each liquid is contained in an 1U cylindrical propellant tank with a 60 g neodymium magnet surrounding its fuel outlet, as shown in Figure 5. The contact angle θ_c, hysteresis parameter Γ and inertial acceleration g are set to be $60°$, 0 (free-edge) and 0 (microgravity), respectively. The magnet is assumed to be magnetized in the vertical direction at 1500 kA/m.

The meniscus profile and magnetic Bond numbers for 40%, 60% and 80% filling ratios are represented in Figure 6. The low magnetic susceptibility of liquid oxygen gives raise to a smooth meniscus profile with limited changes in curvature. In contrast, the combination of low surface tension and high magnetic susceptibility of the methane-based ferrofluid quickly produces a central protrusion. The evolution of the meniscus with the filling ratio is represented in Figure 7, where the FR=30% level detaches from the lateral

Table 1: Physical properties of CH_4 (l) enriched with a 0.53% volume of Fe_3O_4 nanoparticles, and of O_2 (l) at cryogenic storage temperature.[42–45]

Substance	T [K]	P [bar]	ρ [kg/m^3]	σ [mN/m]	χ_{ini}
CH_4(l) + Fe_3O_4(s)	111	2	448	12.99	Fig. 4
O_2(l)	90	2	1141	13.2	0.0042

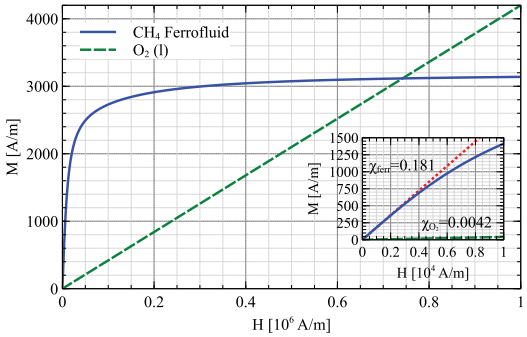

Figure 4: Magnetization curves of liquid CH_4 enriched with a 0.53% volume of Fe_3O_4 nanoparticles (ferromagnetic) and liquid O_2 (paramagnetic)

wall and has been removed and the FR=100% is shown as a reference without considering the top end of the cylindrical container. It is interesting to note how the fluid surface tends to follow the constant Bo_{mag} lines. From the physical viewpoint, this is equivalent to the tendency of an air balloon to equal the pressure over its surface. The roles played by air pressure and membrane tension are here assumed by the magnetic force and surface tension, respectively.

An indication of the reachability of the magnet is obtained by analyzing the constant $Bo_{\text{mag}} = 1$ lines, that define the transition from magnetic to surface-tension dominated regions. While for liquid oxygen this line crosses the symmetry axis at a height of approximately 64 mm, in the case of the ferrofluid the crossing is produced at $z > 100$ mm due to its enhanced magnetic properties. However, the magnetic Bond number depends on the position and should then be analyzed along the meniscus. This analysis in given in Figure 8, that illustrates the previous comments and reflects once more the greater susceptibility of the ferrofluid.

Figure 9 depicts the three first sloshing frequencies for both systems as a function of the filling ratio. While only a slight effect is observed for the O_2 (l) tank, increases of the fundamental frequency between a 18% and a 786% with respect to the non-magnetic case are depicted in the CH_4-based ferrofluid analysis. Ferrofluids may then be particularly well suited for highly demanding magnetic liquid management applications in space, such as active magnetic positive positioning or magnetic sloshing damping. Since liquid oxygen has the highest know paramagnetic susceptibility of pure liquids, this analysis also unveils the limitations non-ferromagnetic liquids for such advanced concepts.

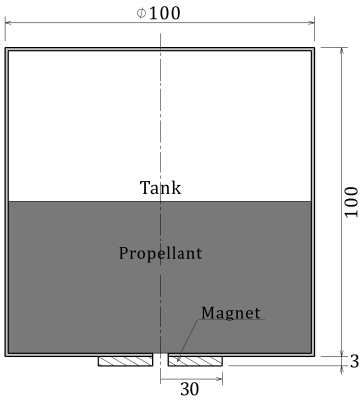

Figure 5: Sketch of the 1U propellant tank considered in the analysis. Units in mm.

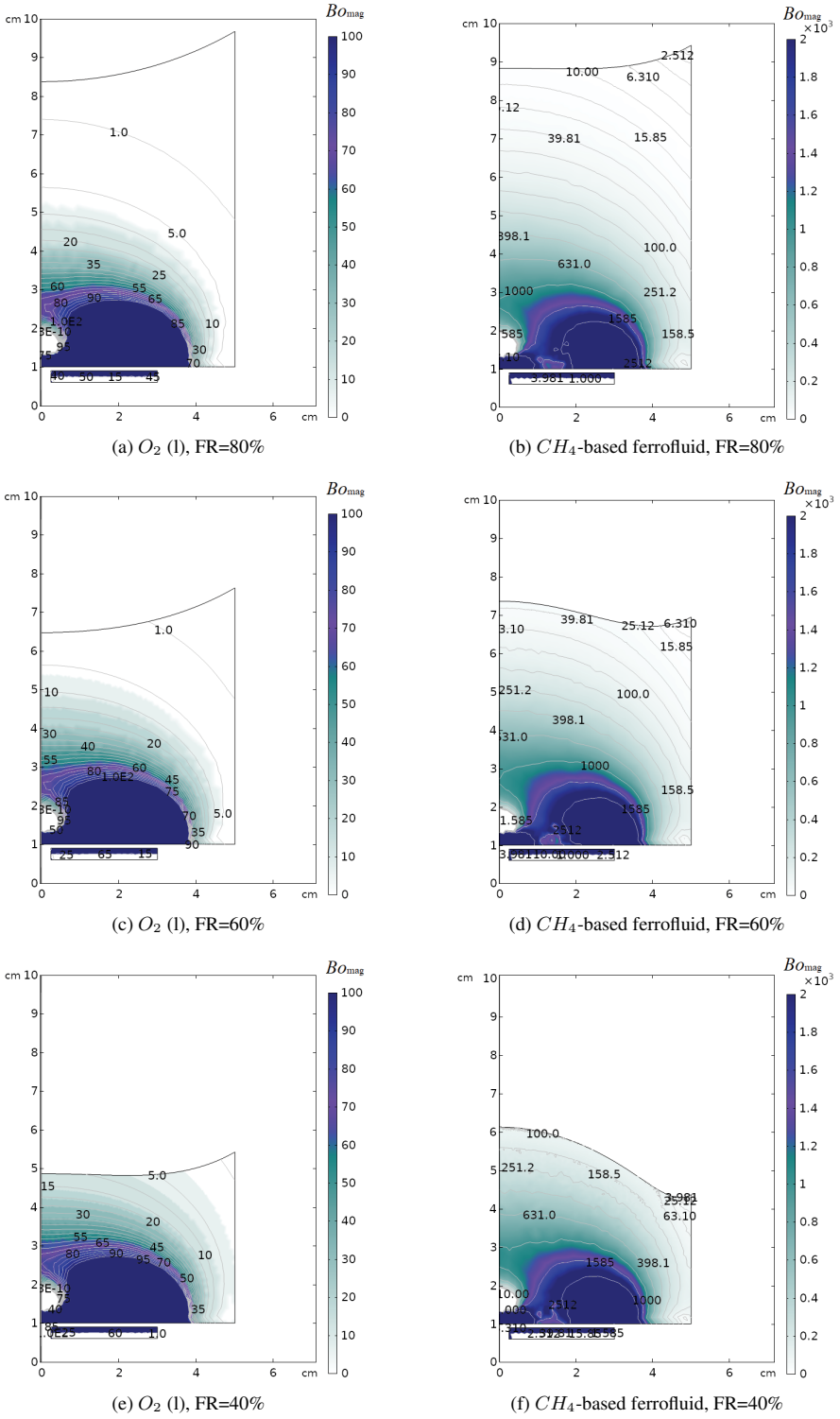

(a) O_2 (l), FR=80%

(b) CH_4-based ferrofluid, FR=80%

(c) O_2 (l), FR=60%

(d) CH_4-based ferrofluid, FR=60%

(e) O_2 (l), FR=40%

(f) CH_4-based ferrofluid, FR=40%

Figure 6: Axisymmetric meniscus profile and magnetic Bond number (color scale) for different filling ratios.

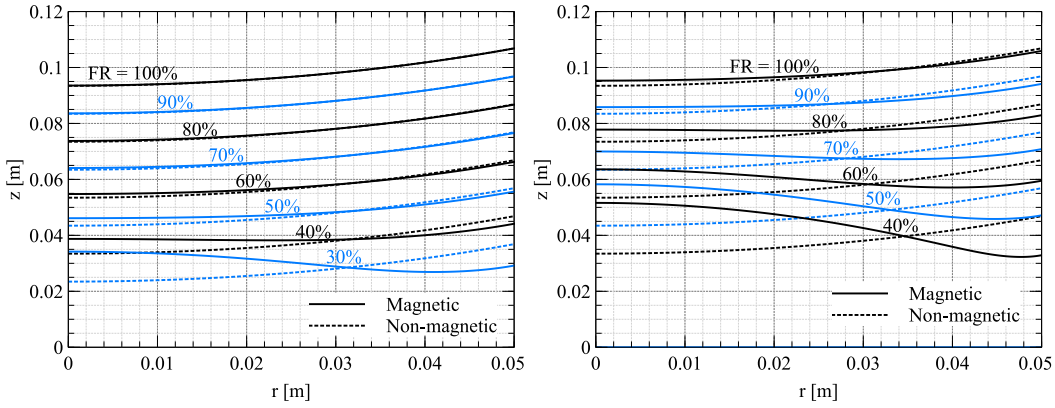

(a) O_2 (l) (b) CH_4-based ferrofluid

Figure 7: Axisymmetric meniscus profile as a function of the filling ratio (FR).

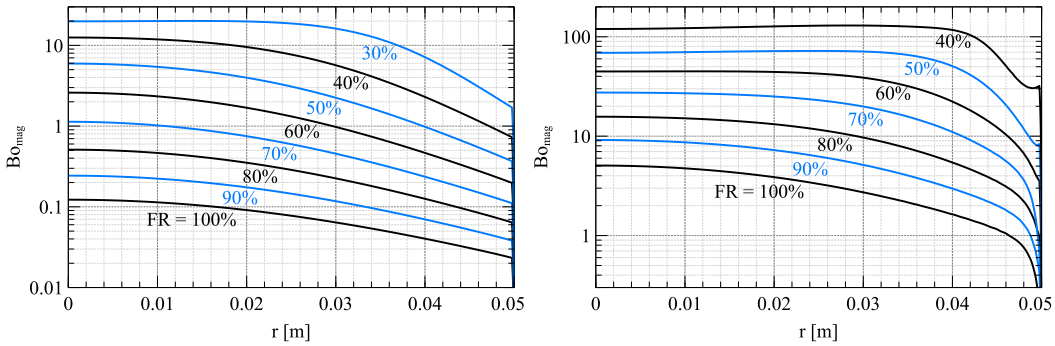

(a) O_2 (l) (b) CH_4-based ferrofluid

Figure 8: Magnetic Bond number at the axisymmetric meniscus as a function of the filling ratio (FR).

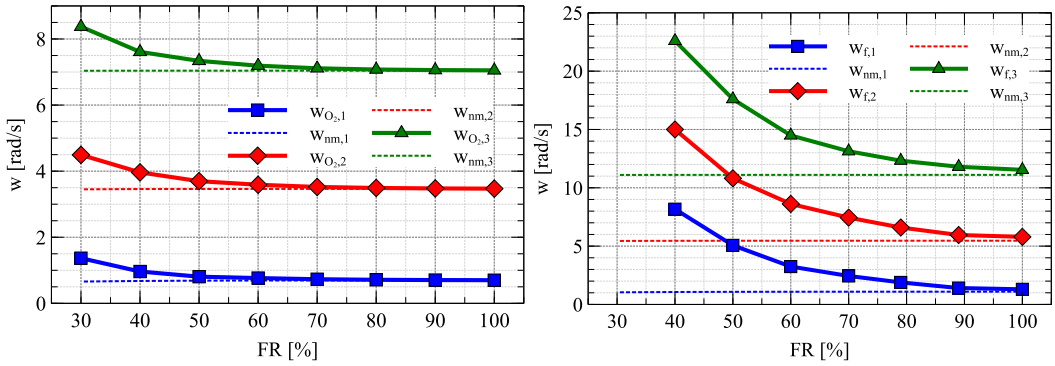

(a) O_2 (l) (b) CH_4-based ferrofluid

Figure 9: Fundamental free-edge sloshing frequencies as a function of the filling ratio (FR).

System scaling

Applications dealing with magnetic propellant positioning[15] or magnetic sloshing control[25] consider either small regions or small propellant tanks due to the rapid decay of magnetic fields. It is reasonable to ask if this concept can be extended to larger tanks, and with which mass penalty.

In order to illustrate the scaling process, a current loop with radius R and current intensity I is subsequently considered. The magnetic field in the symmetry axis is

$$\boldsymbol{B}_{\text{loop}} = \mu_0 \frac{IR^2}{2(z^2+R^2)^{3/2}} \boldsymbol{e}_z, \tag{10}$$

where z is the out-of-plane distance and $\boldsymbol{e}_z$ is the unitary vector along the symmetry axis. Assuming that magnetization and magnetic fields are collinear and neglecting the surface force component (or, equivalently, assuming a small magnetic susceptibility $\chi \ll 1$), the total force per unit volume produced by the loop on an infinitesimal ferrofluid drop located in the symmetry axis is

$$\boldsymbol{F}_m \approx \mu_0 M \frac{\partial H}{\partial z} \boldsymbol{e}_z. \tag{11}$$

Making again use of the assumption $\chi \ll 1$, the magnetic flux density due to the imanation of the ferrofluid can be considered negligible, and hence $\boldsymbol{B} \approx \mu_0 H_0$ inside the drop, with H_0 being the external magnetic field. The internal magnetic field can then be approximated as $\boldsymbol{H} = \boldsymbol{H}_0 - \boldsymbol{M}$. Restricting the analysis to the linear section of the ferrofluid imanation curve, where $\boldsymbol{M} \approx \chi \boldsymbol{H}$, a simplified expression for the total force can be obtained as

$$\boldsymbol{F}_m \approx \mu_0 \frac{\chi}{(1+\chi)^2} H_0 \frac{\partial H_0}{\partial z} \boldsymbol{e}_z. \tag{12}$$

Since $H_0 = \boldsymbol{B}_{\text{loop}}/\mu_0$, the inclusion of Eq. 10 into Eq. 12 results in

$$\boldsymbol{F}_m \approx \mu_0 \frac{\chi}{(1+\chi)^2} \frac{3I^2R^4 z}{4(R^2+z^2)^4} \boldsymbol{e}_z. \tag{13}$$

This expression can be applied to axially magnetized cylindrical magnets with magnetization M_m, radius R and height l by employing an equivalent circular loop with the same radius and current intensity $I = M_m l$.

Equation 13 unveils some important features of the system. The evolution of F_m with z is strongly influenced by R. An increase in the radius of the current loop for constant intensity reduces and increases the force for small and large values of z, respectively. If the mass of the magnet is conserved with the change of R, the new equivalent current intensity becomes $I = M_m l R_0^2/R^2$ and an increase in R reduces the value of F_m for all z. However, the values of F_m outside the symmetry axis benefit from the more homogeneous field generated by wide magnets.

Most importantly, a geometrical scaling of R, l and z by a factor K multiplies F_m by $1/K$. The scaled ferrofluid meniscus would then be subjected to $1/K$ times the original force. Since the magnetic Bond number definition given by Eq. 7 is multiplied by the square of the characteristic length, it turns out that the Bo_{mag} number of the new system is multiplied by K. In other words, an upscaling of the liquid tank requires relatively smaller magnetic sources to produce an equivalent effect on the fluid.

This conclusion is exemplified in Figure 10 by scaling the previously described CH_4 propellant tank by a factor $K = 10$. The radius of the magnet is then reduced from 30 cm to 15 cm to approximately recover the original magnetic Bond number, achieving a 75% mass reduction (45 kg for a magnet density of 7100 kg/m^3). Including the weight of the magnetic nanoparticles and the magnet, the total mass of the magnetic control system is 31 kg, representing a 12% of the propellant mass (282 kg for 80 cm filling height). This value can be significantly reduced with a dedicated optimization process.

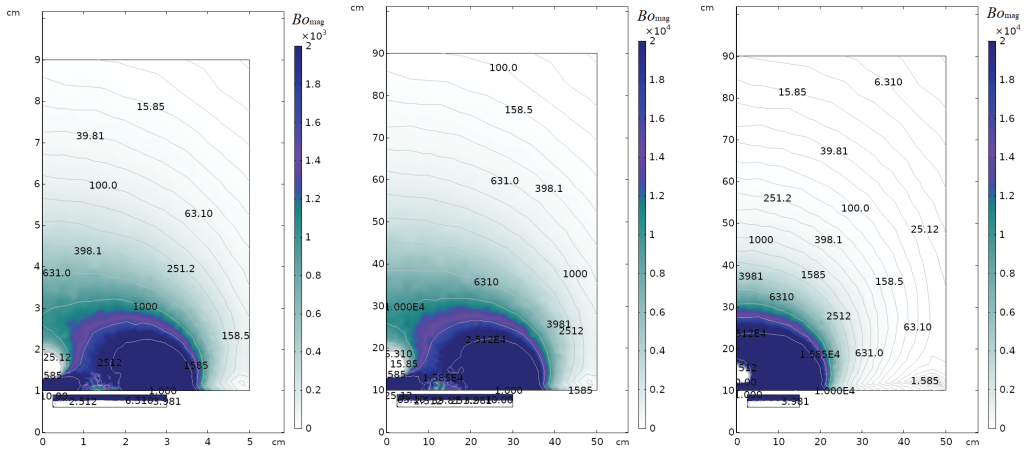

(a) Original tank (b) $K = 10$ scaling (c) Corrected $K = 10$ scaling

Figure 10: Bo_{mag} distribution (color scale) in a CH_4-based ferrofluid with FR=80% and a flat surface.

Stability requirements of ferrofluids

If ferrofluids are sought to be employed for space applications, their long-term stability and resistance to the space environment must be ensured. The physicochemical stability of a colloid is determined by the balance between the energetic contributions of the system. Under specific environmental conditions, a sufficiently small particle will avoid settling (decantation to the sources of potential) and agglomeration (union of several particles) if an appropriate surfactant is employed to overcome the Van der Waals attraction. The excellent discussion on the stability requirements of ferrofluids provided by Rosensweig in Ref. 27 is subsequently summarized and applied for the hypothetical CH_4 ferrofluid under analysis.

The stability against settling by magnetic sources is achieved by imposing a high ratio of thermal to magnetic energy. This gives a first upper boundary to the particle diameter

$$d \leq d^m_{\text{max}} = \left(\frac{6kT}{\pi \mu_0 M H} \right)^{1/3}, \tag{14}$$

where $k = 1.38 \cdot 10^{-23}$ NmK^{-1}, T is the absolute temperature, M is the magnetization field module and H is the magnetic field module. A similar reasoning for the gravitational energy results in

$$d \leq d^g_{\text{max}} = \left(\frac{6kT}{\pi \Delta \rho g L} \right)^{1/3}, \tag{15}$$

with $\Delta\rho = \rho_{\text{solid}} - \rho_{\text{liquid}}$ being the differential density, g the inertial acceleration and L the elevation in the gravitational field. The ratio between gravitational and magnetic energy is

$$\frac{E_g}{E_m} = \frac{\Delta \rho g L}{\mu_0 M H}. \tag{16}$$

Two magnetic particles located sufficiently close will also experience an attractive dipole-dipole force. If this force was left acting alone, the collisions between particles would lead to the rapid agglomeration of the colloid. The energy required to detach a pair of aligned particles is the dipole-dipole contact energy

$$E_{dd} = \frac{1}{12} \mu_0 M^2 V, \tag{17}$$

with $V = \pi d^3/6$ being the volume of the particle. In order to avoid this process, the ratio between thermal and dipole-dipole contact energy must then be greater than unity, leading to the condition

$$d \leq d_{\text{max}}^{dd} = \left(\frac{72kT}{\pi \mu_0 M^2} \right)^{1/3}. \tag{18}$$

The dipole-dipole force acts together with the Van der Waals attraction, always present due to the fluctuating electric dipole-dipole forces. Assuming spherical particles, its associated energy would be

$$E_{V.d.W.} = -\frac{A}{6} \left[\frac{2}{l^2 + 4l} + \frac{2}{(l+2)^2} + \ln \frac{l^2 + 4l}{(l+2)^2} \right] \tag{19}$$

with $l = 2s/d$, s being the surface-to-surface separation distance and A the *Hamaker constant*, approximately equal to 10^{-19} for Fe, Fe_2O_3 or Fe_3O_4 in hydrocarbon. Unlike the magnetic dipole-dipole energy, Eq. 19 diverges when $s \to 0$. In other words, the contact between particles must be physically avoided to prevent agglomeration, as thermal energy is unable to prevent coagulation. The problem can be solved by adding a surfactant layer made of long chain molecules, producing a mechanism known as *steric* or *entropic* repulsion. According to Mackor's theory, such a surfactant produces a repulsive energy of the form[27,48]

$$E_{\text{steric}} = kT \frac{\pi d^2 \xi}{2} \left[2 - \frac{l+2}{t} \ln \left(\frac{1+t}{1+l/2} \right) - \frac{l}{t} \right], \tag{20}$$

where ξ is the surface concentration of absorbed molecules and $t = 2\delta/d$. Alternatively, the particles may be charged to generate a Coulomb repulsion, producing *ionic* ferrofluids.

The agglomeration rate is then determined by the net potential curve, obtained as the difference between attractive and repulsive energies. For very short separation distances the Van der Waals attraction dominates; otherwise, the steric repulsion prevents the contact. Consequently, two given particles collide only when their thermal energy is greater than the maximum of the net potential. If this energy barrier is well designed (i.e. only a negligible portion of the thermal energy histogram overcomes the steric repulsion barrier), the ferrofluid should remain in good condition for long time periods.[27]

Space applications dealing with ferrofluids must carefully consider this trade-off analysis. The mission may expose the liquid to (i) launch accelerations of up to 10 gs, (ii) long-term microgravity conditions, and (iii) significant thermal gradients. In principle, the first two points represent minor concerns, as the time required to change the equilibrium profile of the colloid is several orders of magnitude greater than the high-gravity window[49,50] and the process is reversible.[27] On the contrary, colloids subjected to excessive temperatures experience an accelerated thermal aging leading to sedimentation and the degradation of magnetic properties.[51] This should be considered when exposing the liquid to significant thermal gradients.

For the CH_4-based ferrofluid propellant here considered, $d_{\text{max}}^{m} = 15$ nm, $d_{\text{max}}^{g} = 3$ nm and $d_{\text{max}}^{dd} = 149$ nm for a storage temperature $T = 111$ K, maximum magnetic field $H = 10^5$ A/m, maximum magnetization field 2900 A/m, launch acceleration $g = 98.1$ m/s^2, differential density $\Delta\rho = 7450$ kg/m^3 and elevation length $L = 0.1$ m. The surfactant design is also subjected to other requirements (e.g. resistance to low temperatures and space radiation) and falls beyond the scope of this preliminary analysis. Again, it should be noted that the launch acceleration lasts for few minutes and that the condition $d < d_{\text{max}}^{g}$ may hence be relaxed.

Radiation stability of ferrofluids

Long-term exposure to space radiation may degrade the colloid and modify its magnetic response. The literature on the topic is scarce, focusing mainly on biomedical applications.

Early studies by Kopčanský *et al.* report strong reductions in the initial susceptibility (-40%), saturation magnetization (-25%) and number of magnetic particles (-36%) of kerosene-based ferrofluids after being irradiated with 17.3 Gy of γ-radiation. This degradation is attributed to the destruction of the long polar chain molecules of the stabilizing oleic acid and kerosene. Similar experiments on non-stabilized Fe_3O_4

diester-based ferrofluids show no significant degradation of the magnetization of the Fe_3O_4 nanoparticles. However, a strong influence in the stabilization process is observed.[52] Bădescu *et al.* also report reductions in initial susceptibility and saturation magnetization of a 5-10% in kerosene-based ferrofluids subjected to 5-20 Gy of γ-ray radiation. The same effect is not measured for water-based solutions, attributing this behavior to the superficial anisotropy produced by the implantation of free oleic acid molecules on the particle surface.[53] More recent works with Gd_2O_3-based ferrofluids using CTAB as a surfactant and ethanol as a carrier liquid analyze the development of intragranular defects due to γ-ray radiation levels in the range between 32 Gy and 2635 Gy. Results suggest the existence of a critical dose beyond which the defects would tend to saturate.[54]

The effects of electron irradiation on biocompatible water-based ferrofluids are explored by Tomašovičová *et al.* with natrium oleate and double layer natrium oleate/PEG surfactants in Ref. 55. Stable reductions in saturation magnetization of a 50% and a 25% are respectively measured after applying an irradiation dose of 1000 Gy, although most of the loss is already produced for 5 Gy. PEG is shown to behave as a protective surfactant against radiation, with this capability being independent of its molar weight.[56] The degradation process is attributed to the aggregation of particles produced by ionization. Similar experiments with bovine serum albumin (BSA) modified ferrofluids containing sodium oleate stabilized Fe_3O_4 nanoparticles show a dependence between the w/w BSA/Fe_3O_4 ratio and the stability against radiation.[57]

Studies with a technical and more practical scope have also been presented. Ferrofluid feedthrough (FF) rotary seals are exposed in Ref. 58 to a mixed radiation field consisting of fast neutrons (0.2 MGy), protons (2 MGy) and γ-rays (20 MGy). Serious magneto-viscous damages are reported for radiation levels above 2 MGy. Reference 59 reports the negative impact of a 900 MHz 30 W electromagnetic radiation on the discharging current of transformer oil ITO 100. As a last example, in Ref. 60 microwave heating applied during the synthesis of aqueous ferrofluids is shown to increase the saturation magnetization and have a negligible effect on the stability properties.

This short literature review reflects the high sensitivity of ferrofluids to different kinds of radiation. Their effect is dependent on the selection of nanoparticles, coatings and carrier liquids. Any application of ferrofluids in space must consequently address their long-term chemical stability when exposed to the combined action of space radiation and microgravity. Significant differences between LEO, GEO and deep space orbits should be expected. To the best knowledge of the authors, such analysis still needs to be performed.

Impact of ferrofluid-enriched propellants on the propulsion subsystem

Slurry fuels is a wide class of liquids consisting of a solid phase in the shape of particles, from the submicrometric to some hundreds of micron, suspended in a fluid medium. The use of metal-based particles in liquid propellants has been analyzed since the 1950s with the perspective to enhance ideal propulsion performance.[61] The stabilization of the suspension can be obtained through liquid gelification, treatment with surfactants, use of dispersant etc. Proposed applications considered different fields of the propulsion (from rocket to air breathing) to obtain lighter and more compact systems. Specific impulse and propellant average density augmentation could be obtained, depending on the peculiar properties of the suspended material. As an example, mixtures of aluminum suspended in gelled kerosene, burned in combination with liquid oxygen were targeted by NASA. Palaszewsky and Zakany described the experience on aluminum suspensions in kerosene, showing theoretical and experimental results up to metal loads of 55%.[62] In the reported case, gelification of the suspending medium was necessary to stabilize the dispersion. Known issues connected to the use of metal-based slurry fuels are deposition on nozzle and walls, erosion of injectors, and agglomeration of particles during the combustion process. Lifetime of the slurry became a critical aspect for the real application.

Ferrofluids have been associated to space propulsion since their invention. In 1963 Papell already described colloidal suspensions of magnetite on heptane or JP_4 carriers.[6] Water-based ferrofluids may also find application as high-density propellants for In-Situ-Resource-Utilization (ISRU),[63] and light hydrocarbons are widely employed as carriers in commercial ferrofluids.[27] However, liquid propellant rocket fuels never made use of iron oxide. Iron-based compounds have been used in the past for soot reduction in the combustion of complex hydrocarbons (e.g. diesel, kerosene) whereas studies on behavior with alcanes are mostly reported

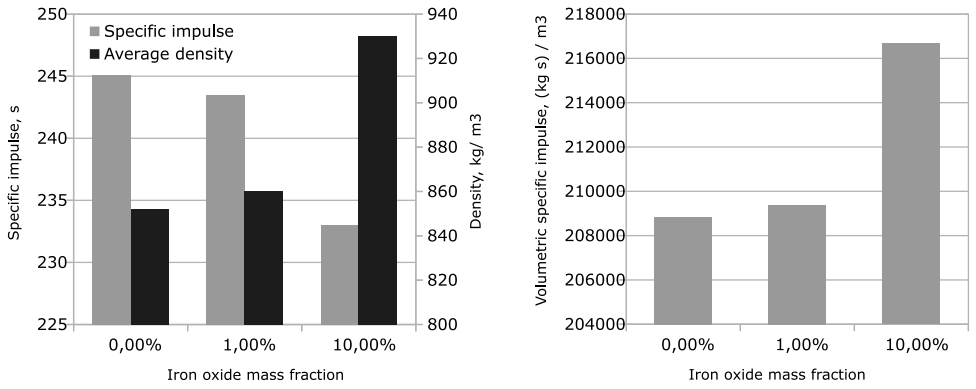

(a) Specific impulse and average density

(b) Volumetric specific impulse

Figure 11: Analysis of the combustion of $LCH_4/LOX/Fe_3O_4$.

for reduction of the oxide.[64] There are different forms of iron oxide and catalytic/decomposition properties depend on the exact molecule. Hematite is the most stable and its stability depends on reaction temperature and atmosphere. The reduction in a methane environment of Fe_2O_3 has been documented by Ghosh and co-authors between 1073 K and 1298 K. Active role is attributed to the molecular hydrogen generated by the decomposition of the CH_4 molecule.[65] This property has been used in chemical looping combustion processes. As an example, in a paper by Monazam iron-based compound acts as oxygen carrier between a section of the reactor where Fe_2O_3 oxidizes a fuel and another part where air oxidizes the resulting metal-based material back to hematite. Reportedly, reaction with methane can generate Fe_3O_4, FeO or Fe depending on the degree of hematite reduction.[66] Out of the iron oxide family, magnetite (Fe_3O_4) is a combination of the two oxidation states Fe(II) and Fe(III). It is an amphoteric compound arranged in mixed octahedral/tetrahedral configuration (inverse spinel). It is featured by ferromagnetic properties and high electric conductivity.[67] For this reason, magnetite is a perfect candidate for ferroluids.

From the rocket propulsion viewpoint, iron oxide is a component characterized by low energy content due to its low formation enthalpy. Thermodynamic computations are reported in Figure 11.[68] The specific impulse is computed for the oxidizer-to-fuel of 4 at 20 bar, nozzle pressure ratio of 20 with optimal discharge and frozen expansion model. Chemical equilibrium is assumed in the combustion chamber only. The evaluations are performed at the reference iron oxide content of 1% and 10% and are compared against a baseline without the oxide additive. As expected, the specific impulse decreases constantly once the iron oxide is introduced. The decrement is less than 1% when Fe_3O_4 fraction is 1% and becomes about 5% for the 10% additive mass concentration. The variation is attributed to the reduction of the flame temperature and the increasing value of the combustion mixture molar mass.[69] Figure 11 reports also the average density of the liquid propellant before combustion. Data are considered for liquid propellants at their respective boiling points. This figure of merit concurs to the definition of the volumetric specific impulse (the product between the specific impulse and the propellant average density) and is important to rate the compactness of a propulsion system.[70] A 1% addition of magnetite generates +1% density and 10% additive content leads to +10% density. This trend attributes a global increase to the volumetric specific impulse showing that the use of ferrofluid dispersed into the propellant can be beneficial from the compactness viewpoint.

CONCLUSIONS

A review of the fundamental theoretical tools required in the modeling and analysis of low-gravity magnetic propellant positioning has been presented. Potential applications in the ambit of space propulsion have been introduced together with their associated technical challenges.

In spite of the theoretical and experimental efforts devoted to the study of magnetic liquid sloshing, fundamental questions still need to be addressed. Among them, the effects of the magnetic interaction on the critical Bond number (Bo^*) and the influence of magnetically-induced viscosity in the frequencies and damping ratios of the system.

Simulations with O_2 (l) and an hypothetical CH_4-based ferrofluid have revealed the strengths and weaknesses of this concept. Due to their small magnetic susceptibility, paramagnetic substances seem to be limited to low-demanding tasks, such as passive MP^2. On the contrary, ferrofluids may be employed on active MP^2 and magnetic sloshing control applications. The magnetic force at the fluid surface, that determines the response of the liquid, grows with $1/K$ for a geometrical scaling factor K. However, the magnetic Bond number is proportional to K. This implies that larger tanks require relatively smaller magnetic sources to induce an equivalent effect on the fluid, and hence lower relative masses. The question remains whether the increase of Bo^* is enough to satisfy the stability requirements of specific space missions, and if the benefits compensate the cost.

The technical challenges associated to the employment of ferrofluid-based space propellants have also been explored. The stability of such solutions must be guaranteed against thermal and radiation-induced aging. Although of fundamental importance, the effects of space radiation on ferrofluids seems to be completely unexplored. Finally, it has been shown how the addition of Fe_2O_3 nanoparticles to the combustion of O_2 and CH_4 produces a slight decrease of specific impulse and an increase of volumetric specific impulse. This can be beneficial from the compactness viewpoint.

ACKNOWLEDGMENTS

The authors thank Dr Gabriel Cano Gómez for his academic assistance, and Dr Daniel Kubitschek for contributing to the initial discussions that motivated this manuscript. The financial support offered by the *La Caixa* Foundation in the framework of the *La Caixa* Fellowship Program is acknowledged.

REFERENCES

[1] M. Eswaran and U. K. Saha, "Sloshing of liquids in partially filled tanks - a review of experimental investigations," *Ocean Systems Engineering*, Vol. 1, No. 2, 2011.

[2] W. C. Reynolds and H. M. Satterlee, *The Dynamic Behavior of Liquids in Moving Containers*. NASA SP-106, 1966.

[3] F. Dodge, *The New Dynamic Behavior of Liquids in Moving Containers*. Southwest Research Institute, 2000.

[4] A. Y. Lee and J. Stupik, "In-Flight Characterization of the Cassini Spacecraft Propellant Slosh Modes," *Journal of Spacecraft and Rockets*, Vol. 54, No. 2, 2017, pp. 417–425, 10.2514/1.A33636.

[5] D. Chipchark, "Development of expulsion and orientation systems for advanced liquid rocket propulsion systems," *USAF Technical Report RTD-TDR-63-1048, Contract AF04 (611)-8200*, 1963.

[6] S. Papell, "Low viscosity magnetic fluid obtained by the colloidal suspension of magnetic particles," *US Patent 3215572*, 1963.

[7] S. Kaneko, T. Ishiyama, and T. Sawada, "Effect of an applied magnetic field on sloshing pressure in a magnetic fluid," *Journal of Physics: Conference Series*, Vol. 412, No. 1, 2013, p. 012018.

[8] M. Ohaba and S. Sudo, "Liquid surface behavior of a magnetic liquid in a container subjected to magnetic field and vertical vibration," *Journal of Magnetism and Magnetic Material*, Vol. 149, 1995, pp. 38–41.

[9] S. Sudo, H. Nishiyama, K. Katagiri, and J. Tani, "Interactions of Magnetic Field and the Magnetic Fluid Surface," *Journal of Intelligent Material Systems and Structures*, Vol. 10, No. 6, 1999, pp. 498–504.

[10] T. Ishiyama, S. Kaneko, S. Takemoto, and T. Sawada, "Relation between Dynamic Pressure and Displacement of Free Surface in Two-Layer Sloshing between a Magnetic Fluid and Silicone Oil," *Materials Science Forum*, 2014.

[11] T. Sawada, Y. Ohira, and H. Houda, "Sloshing motion of a magnetic fluid in a cylindrical container due to horizontal oscillation," *Energy Conversion and Management*, Vol. 43, No. 3, 2002, pp. 299–308.

[12] K. Ohno, M. Shimoda, and T. Sawada, "Optimal design of a tuned liquid damper using a magnetic fluid with one electromagnet," *Journal of Physics: Condensed Matter*, Vol. 20, No. 20, 2008, p. 204146.

[13] K. Ohno, H. Suzuki, and T. Sawada, "Analysis of liquid sloshing of a tuned magnetic fluid damper for single and co-axial cylindrical containers," *Journal of Magnetism and Magnetic Materials*, Vol. 323, No. 10, 2011, pp. 1389 – 1393. Proceedings of 12th International Conference on Magnetic Fluid, Sendai, Japan.

[14] F. T. Dodge and L. R. Garza, "Free-Surface Vibrations of a Magnetic Liquid," *Journal of Engineering for Industry*, Vol. 94, No. 1, 1972, pp. 103–108.

[15] J. Martin and J. Holt, "Magnetically Actuated Propellant Orientation Experiment, Controlling fluid Motion With Magnetic Fields in a Low-Gravity Environment," *NASA/TM-2000-210129, M-975, NAS 1.15:210129*, 2000.

[16] J. Marchetta and J. Hochstein, "Fluid capture by a permanent ring magnet in reduced gravity," *Proceedings of the 37th Aerospace Sciences Meeting and Exhibit, Reno, NV, USA*, American Institute of Aeronautics and Astronautics, 1999.

[17] J. Marchetta and J. Hochstein, "Simulation and dimensionless modeling of magnetically induced reorientation," *Proceedings of the 38th Aerospace Sciences Meeting and Exhibit, Renno, NV, USA*, American Institute of Aeronautics and Astronautics, 2000.

[18] J. Marchetta, J. Hochstein, D. Sauter, and B. Simmons, "Modeling and prediction of magnetic storage and reorientation of LOX in reduced gravity," *40th AIAA Aerospace Sciences Meeting & Exhibit*, American Institute of Aeronautics and Astronautics, 2002.

[19] J. G. Marchetta, "Simulation of LOX reorientation using magnetic positive positioning," *Microgravity - Science and Technology*, Vol. 18, Mar 2006, p. 31, 10.1007/BF02908417.

[20] J. Marchetta and A. Winter, "Simulation of magnetic positive positioning for space based fluid management systems," *Mathematical and Computer Modelling*, Vol. 51, No. 9, 2010, pp. 1202 – 1212.

[21] A. Romero-Calvo, T. H. Hermans, G. C. Gómez, L. P. Benítez, M. H. Gutiérrez, and E. Castro-Hernández, "Ferrofluid Dynamics in Microgravity Conditions," *Proceedings of the 2nd Symposion on Space Educational Activities, Budapest, Hungary*, 2018.

[22] A. Romero-Calvo, T. H. Hermans, L. P. Benítez, and E. Castro-Hernández, *Drop Your Thesis! 2017 Experiment Report - Ferrofluids Dynamics in Microgravity Conditions*. European Space Agency - Erasmus Experiment Archive, 2018.

[23] A. Romero-Calvo, A. García-Salcedo, I. Rivoalen, F. Garrone, G. C. Gomez, E. Castro-Hernández, M. H. Gutiérrez, and F. Maggi, "Lateral Sloshing of Magnetic Liquids in Microgravity," *Proceedings of the 70th International Astronautical Congress, Washington DC, USA*, 2019.

[24] A. Romero-Calvo, A. García-Salcedo, F. Garrone, I. Rivoalen, G. C. Gomez, E. Castro-Hernández, and F. Maggi, "Free Surface Reconstruction of Opaque Liquids for Experimental Sloshing Analyses in Microgravity," *Proceedings of the 70th International Astronautical Congress, Washington DC, USA*, 2019.

[25] A. Romero-Calvo, G. Cano Gómez, E. Castro-Hernández, and F. Maggi, "Free and Forced Oscillations of Magnetic Liquids Under Low-Gravity Conditions," *Journal of Applied Mechanics*, Vol. 87, 12 2020. 021010, 10.1115/1.4045620.

[26] A. Myshkis and R. Wadhwa, *Low-gravity fluid mechanics: mathematical theory of capillary phenomena*. Springer, 1987.

[27] R. E. Rosensweig, *Ferrohydrodynamics*. Dover Publications, 1997.

[28] J. L. Neuringer and R. E. Rosensweig, "Ferrohydrodynamics," *The Physics of Fluids*, Vol. 7, No. 12, 1964, pp. 1927–1937.

[29] M. Petit, A. Kedous-Lebouc, Y. Avenas, M. Tawk, and E. Arteaga, "Calculation and analysis of local magnetic forces in ferrofluids," *Przeglad Elektrotechniczny (Electrical Review)*, Vol. 87, 2011, pp. 115–119.

[30] M. Liu and K. Stierstadt, "Electromagnetic Force and the Maxwell Stress Tensor in Condensed System," *Condensed Matter*, 2000.

[31] S. Odenbach and M.Liu, "Invalidation of the Kelvin Force in Ferrofluids," *Physical Review Letters*, Vol. 86, 2001, p. 328.

[32] A. Romero-Calvo, G. Cano-Gómez, T. H. Hermans, L. P. Benítez, M. A. Herrada-Gutiérrez, and E. Castro-Hernández, "Total magnetic force on a ferrofluid droplet in microgravity," *Manuscript submitted for publication.*, 2019.

[33] H. M. Satterlee and W. C. Reynolds, "The Dynamics of Free Liquid Surface in Cylindrical Containers Under Strong Capillary and Weak Gravity Conditions," *Stanford University Mechanical Engineering Department*, Vol. Report LG-2, 1964.

[34] G. Yeh, "Free and Forced Oscillations of a Liquid in an Axisymmetric Tank at Low-Gravity Environments," *Journal of Applied Mechanics*, 1967.

[35] M. Shliomis, "Effective Viscosity of Magnetic Suspensions," *Soviet Physics JETP*, Vol. 34, 1972, pp. 1291–1294.

[36] J. P. Shen and M. Doi, "Effective Viscosity of Magnetic Fluids," *Journal of the Physical Society of Japan*, Vol. 59, No. 1, 1990, pp. 111–117, 10.1143/JPSJ.59.111.

[37] A. Causevica, P. Sahli, F. Hild, K. Grunwald, M. Ehresmann, and G. Herdrich, "PAPELL: Interaction Study of Ferrofluid with Electromagnets of an Experiment on the International Space Station," 2018.

[38] D. Ludovisi, S. S. Cha, N. Ramachandran, and W. M. Worek, "Heat transfer of thermocapillary convection in a two-layered fluid system under the influence of magnetic field," *Acta Astronautica*, Vol. 64, No. 11, 2009, pp. 1066 – 1079.

[39] A. Bozhko and G. Putin, "Thermomagnetic Convection as a Tool for Heat and Mass Transfer Control in Nanosize Materials Under Microgravity Conditions," *Microgravity Science and Technology*, Vol. 21, Jan 2009, pp. 89–93.

[40] B. A. Jackson, K. J. Terhune, and L. B. King, "Ionic liquid ferrofluid interface deformation and spray onset under electric and magnetic stresses," *Physics of Fluids*, Vol. 29, No. 6, 2017, p. 064105.

[41] K. Lemmer, "Propulsion for CubeSats," *Acta Astronautica*, Vol. 134, 2017, pp. 231 – 243.

[42] R. J. Meier, C. J. Schinkel, and A. d. Visser, "Magnetisation of condensed oxygen under high pressures and in strong magnetic fields," *Journal of Physics C: Solid State Physics*, Vol. 15, feb 1982, pp. 1015–1024, 10.1088/0022-3719/15/5/019.

[43] G. D. Grayson, M. L. Hand, and E. C. Cady, "Thermally Coupled Liquid Oxygen and Liquid Methane Storage Vessel," US Patent 7,568,352 B2, Aug, 4 2009.

[44] J. M. Jurns and J. W. Hartwig, "Liquid Oxygen Liquid Acquisition Device Bubble Point Tests with High Pressure LOX at Elevated Temperatures," 2011.

[45] C. Wohlfarth, "Surface tension of methane: Datasheet from Landolt-Börnstein - Group IV Physical Chemistry · Volume 24: "Supplement to IV/16"," 2008, 10.1007/978-3-540-75508-1˙20.

[46] E. A. Hulbert, R. Whitley, M. D. Klem, W. Johnson, L. Alexander, E. D'Aversa, J.-M. Ruault, and C. Manfletti, "International Space Exploration Coordination Group Assessment of Technology Gaps for LOx/Methane Propulsion Systems for the Global Exploration Roadmap," 2016.

[47] M. Utsumi, "Mechanical Models of Low-Gravity Sloshing Taking Into Account Viscous Damping," *Journal of Vibration and Acoustics*, Vol. 136, 10 2013. 011007, 10.1115/1.4025439.

[48] E. Mackor, "A theoretical approach of the colloid-chemical stability of dispersions in hydrocarbons," *Journal of Colloid Science*, Vol. 6, No. 5, 1951, pp. 492 – 495, https://doi.org/10.1016/0095-8522(51)90019-0.

[49] E. A. Elfimova, A. O. Ivanov, E. V. Lakhtina, A. F. Pshenichnikov, and P. J. Camp, "Sedimentation equilibria in polydisperse ferrofluids: critical comparisons between experiment, theory, and computer simulation," *Soft Matter*, Vol. 12, 2016, pp. 4103–4112, 10.1039/C6SM00304D.

[50] B. Luigjes, D. M. E. Thies-Weesie, A. P. Philipse, and B. H. Erné, "Sedimentation equilibria of ferrofluids: I. Analytical centrifugation in ultrathin glass capillaries," *Journal of Physics: Condensed Matter*, Vol. 24, may 2012, p. 245103, 10.1088/0953-8984/24/24/245103.

[51] J. Kurimský, M. Rajňák, P. Bartko, K. Paulovičová, R. Cimbala, D. Medveď, M. Džamová, M. Timko, and P. Kopčanský, "Experimental study of AC breakdown strength in ferrofluid during thermal aging," *Journal of Magnetism and Magnetic Materials*, Vol. 465, 2018, pp. 136 – 142, https://doi.org/10.1016/j.jmmm.2018.05.083.

[52] P. Kopčanský, J. Černák, T. Tima, A. Zentko, M. Timko, and P. Slančo, "γ-Radiation induced sedimentation of magnetic particles in magnetic fluids," *Journal of Magnetism and Magnetic Materials*, Vol. 85, No. 1, 1990, pp. 103 – 106, https://doi.org/10.1016/0304-8853(90)90030-T.

[53] V. Badescu, V. Craciun, and G. Calugaru, "The effect of irradiation on the properties of some ferrofluids used in hyperthermia," *2002 IEEE International Magnetics Conference (INTERMAG)*, April 2002, pp. FU7–, 10.1109/INTMAG.2002.1001376.

[54] M. Devi, N. Paul, D. Mohanta, and A. Saha, "Characteristic spectroscopic properties of γ-irradiated rare-earth oxide-based ferrofluids," *Journal of Experimental Nanoscience*, Vol. 7, No. 5, 2012, pp. 586–595, 10.1080/17458080.2010.548408.

[55] N. Tomašovičová, V. Závišová, J. Kováč, M. Koneracká, M. Timko, I. Haysak, M. Koneracká, V. Zavisova, P. Kopčanský, I. Haysak, A. Okunev, A. Parlag, and A. Fradkin, "Radiation stability of biocompatibile magnetic fluid," 2010.

[56] N. Tomašovičová, I. Haysak, M. Koneracká, J. Kováč, M. Timko, V. Závišová, A. Okunev, A. Parlag, A. Fradkin, V. Sakhno, and P.Kopčanský, "Magnetic Properties of Biocompatible Magnetic Fluid after Electron Irradiation," *Proceedings of the European Conference Physics of Magnetism 2011 (PM-11), Poznań*, Vol. 121, June 2012, pp. 1302–1304, 10.12693/APhysPolA.121.1302.

[57] N. Tomašovičová, I. Haysak, J. Kováč, M. Kubovčíková, V. Závišová, M. Timko, A. Okunev, A. Zorkovská, and P.Kopčanský, "Radiation Stability of the BSA Modified Biocompatible Magnetic Fluid," *Proceedings of the 15th Czech and Slovak Conference on Magnetism, Košice, Slovakia*, Vol. 126, June 2014, pp. 262–263, 10.12693/APhysPolA.126.262.

[58] N. Simos, S. Fernandes, W. Mittig, F. Pellemoine, M. Avilov, M. Kostin, L. Mausner, R. Ronningen, M. Schein, and G. Bollen, "Performance degradation of ferrofluidic feedthroughs in a mixed irradiation field," *Nuclear Instruments and Methods in Physics Research Section A: Accelerators, Spectrometers, Detectors and Associated Equipment*, Vol. 841, 2017, pp. 144 – 155, https://doi.org/10.1016/j.nima.2016.10.007.

[59] M. Pavlík, L. Kruželák, M. Mikita, M. Špes, S. Bucko, L. Lisoň, M. Kosterec, L. Beňa, and P. Liptai, "The impact of electromagnetic radiation on the degradation of magnetic ferrofluids," *Archives of Electrical Engineering*, Vol. vol. 66, No. No 2 June, 2017, 10.1515/aee-2017-0027.

[60] S. Bhattacharya, K. Jenamoni, and S. Nayar, "Stability of biomimetic ferrofluids established by a systematic study using microwave irradiation at defined wattages," *Journal of Magnetism and Magnetic Materials*, Vol. 324, No. 20, 2012, pp. 3261 – 3266, https://doi.org/10.1016/j.jmmm.2012.05.001.

[61] P. R. Choudhury, "Slurry fuels," *Progress in Energy and Combustion Science*, Vol. 18, No. 5, 1992, pp. 409 – 427, https://doi.org/10.1016/0360-1285(92)90008-O.

[62] B. Balaszewsky and J. Zakany, "Metallized Gelled Propellants: Oxygen/RP-1/aluminum Rocket Combustion Experiments," Vol. AIAA Paper 95-2435, 1995.

[63] K. P. Doyle and M. A. Peck, "Water Electrolysis Propulsion as a Case Study in Resource-Based Spacecraft Architecture (February 2020)," *IEEE Aerospace and Electronic Systems Magazine*, Vol. 34, Sep. 2019, pp. 4–19, 10.1109/MAES.2019.2923312.

[64] P. Stelmachowski, A. Kopacz, P. Legutko, P. Indyka, M. Wojtasik, L. Ziemiański, G. Żak, Z. Sojka, and A. Kotarba, "The role of crystallite size of iron oxide catalyst for soot combustion," *Catalysis Today*, Vol. 257, 2015, pp. 111 – 116. Air and Water Pollution Abatement Catalysis (AWPAC 2014), https://doi.org/10.1016/j.cattod.2015.02.018.

[65] D. GHOSH, A. K. ROY, and A. GHOSH, "Reduction of Ferric Oxide Pellets with Methane," *Transactions of the Iron and Steel Institute of Japan*, Vol. 26, No. 3, 1986, pp. 186–193, 10.2355/isijinternational1966.26.186.

[66] E. R. Monazam, R. W. Breault, R. Siriwardane, G. Richards, and S. Carpenter, "Kinetics of the reduction of hematite (Fe2O3) by methane (CH4) during chemical looping combustion: A global mechanism," *Chemical Engineering Journal*, Vol. 232, 2013, pp. 478 – 487, https://doi.org/10.1016/j.cej.2013.07.091.

[67] F. Maggi, S. Dossi, C. Paravan, L. Galfetti, R. Rota, S. Cianfanelli, and G. Marra, "Iron oxide as solid propellant catalyst: A detailed characterization," *Acta Astronautica*, Vol. 158, 2019, pp. 416 – 424, https://doi.org/10.1016/j.actaastro.2018.07.037.

[68] S. Gordon and B. McBride, "Computer Program for Calculation of Complex Chemical Equilibrium Compositions and Applications," *NASA Reference Publication*, Vol. RP-1311, 1994.

[69] I. Glassman and R. Sawyer, *The performance of chemical propellants*. AGARDograph ; no.129, Technivision Services, Slough, England, 1970.

[70] G. Sutton and O. Biblarz, *Rocket Propulsion Elements*. John Wiley & Sons, seventh ed., 2007.